Cancer-driven IgG promotes the development of castration-resistant Prostate Cancer though the SOX2-CIgG pathway

Caipeng Qin
Peking University People`s Hospital
Zhengzuo Sheng
Peking Unversity People`s Hospital
Xinmei Huang
Peking University Health Science Centre
Jingshu Tang
Peking University Health Science Centre
Yang Liu
Peking University Health Science Centre
Tao Xu (xutao@pkuph.edu.cn)
Peking University People's Hospital
Xiaoyan Qiu
Peking University Health Science Centre

Research

Keywords: CIgG, CRPC, ADT, SOX2

Posted Date: May 28th, 2020

DOI: https://doi.org/10.21203/rs.3.rs-31159/v1

Abstract

Background:

Although Androgen deprivation therapy (ADT) is the initial treatment strategy for prostate cancer, recurrent castration-resistant prostate cancer (CRPC) eventually ensues. In this study, cancer-derived immunoglobulin G(CIgG) was found to be induced after ADT, identifying CIgG as a potential CRPC driver gene.

Methods:

The expression of CIgG and its clinical significance in prostate cancer tissue was analyzed by TCGA database and immunohistochemistry. Subsequently, the sequence features of prostate cell line (LNcap, DU145, PC3) VHDJH rearrangements were analyzed via comparison with the best matching functional germline IgVH, IgDH and IgJH genes. We also assessed the effect of CIgG on the migratory, invasive and proliferative abilities of prostate cancer cells in vitro and vivo. Cells with high CIgG expression ($CIgG^{high}$) and low CIgG expression ($CIgG^{-/low}$) from the PC3 cell line were sorted by FACS using a CIgG monoclonal antibody named RP215, then, suspended microsphere, colony formation and drug-resistant assays were performed. A NOD/SCID mouse tumor xenograft model was developed for the study of the tumorigenic effects of the different cell populations. The AR-SOX2-CIgG signaling pathway was validated by immunohistochemistry, immunofluorescence, qRT-PCR, Western blot, luciferase and ChIP assays and bioinformatics analyses. Finally, we investigated the effect of RP215 inhibition on the progression of prostate cancer in vivo using a Babl/c nude mouse xenograft model.

Results:

We demonstrated that CIgG was induced by androgen deprivation therapy (ADT) and upregulated by SOX2 [SRY (sex determining region Y)-box 2] in prostate cancer, which may promote the development of CRPC. In addition, our findings underscore a novel role of CIgG signaling in the maintenance of stemness and the progression of cancer through MARK/ERK and AKT in prostate cancer.

Conclusion:

Our data suggests that CIgG could be a driver of CRPC development, and that targeting the SOX2-CIgG axis may therefore inhibit CRPC development after ADT.

1. Background

Prostate cancer (PCa) is largely dependent on androgens, which fuels tumor survival, and ADT has become the standard treatment for locally advanced or metastatic PCa. However, despite initial responses, most PCa cases eventually recur after first-line ADT as CRPC. Although the current therapies for CRPC, for example, chemotherapy based on docetaxel or next-generation androgen receptor pathway inhibitors (ARPIs) such as enzalutamide (ENZ) and abiraterone (ABI), extend survival, durable complete

responses are rare and these therapies also eventually fail[1, 2]. Therefore, identifying unrecognized molecular mechanisms that are induced by ADT and drive the development of CRPC is critical, and could lead to more curative therapies for CRPC.

Immunoglobulins (Igs) are a family of immune molecules that play essential roles in immunne responses. In recent decades, our laboratory and other research groups have revealed that cancer cells can also express Ig, and this specific type of Ig is called cancer-derived immunoglobulin G (CIgG)[3–9]. Fortunately, A monoclonal antibody called RP215 recognizes glycosylated epitope of the CIgG heavy chain with little cross-reactivity to B-cell-derived Ig[10], therefore providing an unparalleled advantage over regular anti-human IgG antibodies in studying CIgG. Related studies revealed that CIgG contributes to the malignant behaviors of cancer cells by displaying stem cell-like features[3, 11, 12] and prompting EMT which casuses metastasis. Interestingly, our studies also demonstrated that CIgG can be induced by ADT, and we hypothesized that CIgG can participate in the oncogenic network which is suppressed by AR signaling.

An earlier study demonstrated that ADT increases the expression of SOX2. Herein, we assume that CIgG is a novel factor regulated by the AR-SOX2 signaling pathway. CIgG is associated with the malignant behavior of prostate cancer, and its overexpression induced by ADT can promote the development of CRPC by increasing the activity of MARK/ERK and AKT which are well-established drivers of CRPC[13–16]. In addition, several lines of evidence have connected the epithelial-to-mesenchymal transition (EMT) to CIgG, Finally, using a Babl/c nude mouse xenograft model, we demonstrate that RP215 inhibits the tumor progression of PCa in vivo.

Collectively, our studies reveal a novel AR-SOX2-CIgG pathway that promotes the development of CRPC. We propose that CIgG is an attractive biomarker and therapeutic target for PCa.

2. Materials And Methods

2.1. Tissue microarrays, samples and immunohistochemistry analysis

A tissue microarray (TMA) was obtained from Shanghai Outdo Biotech (Shanghai, China), this TMA consisted of 72 primary tumors (Gleason score was available in 66 cases) and 5 normal prostate tissues. In addition, 19 primary tumor samples, were obtained from the BioBank of Peking University People's Hospital and used for immunohistochemical analysis. In summary, 91 primary tumor cases, and 5 normal tissue cases, with valid information were used for the IHC analysis in Fig. 1B-D. Another 5 patient-matched pre-ADT biopsies and 5 post-ADT prostatectomy specimens were detected by immunohistochemistry (Fig. 4A). The procedures for IHC staining and calculation of CIgG staining scores have been described previously[17], Low CIgG expression was defined as a score of 0–3, and high expression was defined as a score of 4–9.

2.2. Cell culture and reagents

The prostate cancer cell lines LNcap, C4-2, PC3, DU145, and 293T were obtained from ATCC and maintained by Peking University People`s Hospital. 293T cells and prostate cancer cell lines were cultured in Dulbecco's modified Eagle medium (DMEM) (HyClone, Logan, UT, USA) and minimum essential medium (HyClone), RPMI 1640 (Gibco) respectively in a humidified atmosphere of 5% CO2 at 37 °C, supplemented with 10% FBS (HyClone) and 1% penicillin-streptomycin (HyClone). All cell lines used in this study were regularly authenticated by morphologic observation and confirmed to be free of mycoplasma contamination.

3.3. Cell migration and invasion assays

Cell migration and invasion were evaluated using Transwell invasion assays with or

without Matrigel. To assess the effect of CIgG on cell migration and invasion, 1×10^5 cells were plated into the upper chamber of a 24-well Transwell or Matrigel chamber with 8-μm pores (Corning, NY, USA). For cell migration assays, PC3 and DU145 cells were incubated for 18 h prior to the assay. For cell invasion assays, PC3 and DU145 cells were incubated for 24 h. The nonmigrating cells were removed from the upper surface of the membrane. The cells on the lower surface of the wells were stained with 1% crystal violet and counted in 6 randomly selected microscopic fields (200 × magnification).

3.4. CCK-8 assays

The effect of CIgG on cell proliferation was evaluated using the Cell Counting Kit-

8(CCK-8) assay (Dojindo, Kumamoto, Japan). Briefly, 2,000 cells in 150 μl of medium were seeded onto 96-well plates. The absorbance of each well at 450 nm was measured at five different time points. Prior to all absorbance measurements, the medium in each well was replaced with 100 μl of complete medium supplemented with 10% CCK-8 solution, and the cells were incubated for 2 h.

3.5. Colony formation assays

Cells were plated in 6-well plates at a density of 500 cells per well and cultured for

2 weeks. Then, the colonies were fixed with 4% paraformaldehyde for 20 min, stained

with a 0.5% crystal violet solution for 20 min, and counted.

3.6. Xenograft tumor model

The animal studies were approved by the Institutional Committee of Peking University

People's Hospital. Male NOD/SCID and BALB/c nude mice that were 4–6 weeks old were obtained from Beijing Vital River Laboratory Animal Technology Co., Ltd. (Beijing, China). The mice were allowed to acclimate for 1 week after arrival. For the tumorigenicity assays, male BALB/c nude mice were

subcutaneously injected with 1×10^6 ClgG shRNA vector-transfected PC3 cells in 50% Matrigel (BD Biosciences).

The cultured PC3 cells were stained using RP215, and $ClgG^{High}$ or $ClgG^{-/low}$ cells were sorted by FACS. Five hundred cells $ClgG^{High}$ or $ClgG^{-/low}$ cells were transplanted subcutaneously into the mammary fat pads of NOD/SCID mice (Vital River, Beijing, China) in 50% Matrigel (BD Biosciences). After 5 weeks, the NOD/SCID mice were sacrificed and the number of tumors formed was measured.

For RP215 treatment, BALB/c nude mice were injected with PC3 cells for 20 days, and then the mice were sacrificed. The tumors were sliced into $2 \times 2 \times 2$ mm^3 fragments in sterile dishes containing RPMI 1640. Typically, each fragment was implanted into a subcutaneous area in the right flanks. After one week, the mice were treated with 5 mg/kg RP215 or mIgG as the control by injection around the tumor once every two days. The tumor size was measured every other day, with calipers, and the tumor volume was calculated as follows: $(width^2 \times length)/2$.

3.7. Sequencing and analysis of rearranged genes.

The procedures were described previously[18], The repertoire of the cancer-derived Ig V genes was compared with that of published B-cell-derived Ig V genes[8].

3.8. ChIP assay

Chromatin-IP protocols were adapted from previously reported methods [15]. Briefly, cells were cross-linked with 1% formaldehyde at room temperature for 10 minutes and the reaction was quenched by 0.125 M glycine in PBS for 5 minutes at room temperature. Cells were then washed with ice-cold PBS twice, and incubated with cell lysis buffer and nuclear lysis buffe. Chromatin was sonicated and fragmented to a size of 200–500 bp, precleared with protein G beads, and incubated with 3–5 mg of anti-AR antibodies overnight. Protein-DNA complexes were precipitated, washed, and eluted. Finally, immunoprecipitated DNA fragments were extracted by DNA extraction kits (Magen) and subjected to Q-RT-PCR. The ChIP-PCR primers used are listed in Supplementary Table 3.

3.9. Luciferase assay

The pGL3-Basic plasmid (Promega) was used as a backbone for luciferase reporter construction. Briefly, the ClgG promoter region was cloned by PCR with primers listed in Supplementary Table 3. For the dual luciferase reporter assay, 293T cells were seeded into 24-well culture plates (50000 cells/well) in triplicate for each experimental condition. A total of 0.625 μg of luciferase reporter and 62.5 ng of pRL-TK vector (Promega) with or without 0.625 μg of pEnter-AR were transfected together by using Lipofectamine 3000 (Thermo Fisher). A dual luciferase reporter assay was performed using the Dual-Luciferase Reporter Assay System (Promega) following the manufacturer's instructions. Luciferase activity was measured using the Microplate Luminometer Reader (Veritas Model #9100-002). Transfection efficiency was normalized to Renilla luciferase activity.

3.10. Statistical analyses

Statistical analyses were conducted using the SPSS 22.0 package or GraphPad Prism 7.0. Data are presented as the mean ± standard error of the mean (SEM). The CIgG expression between groups was analyzed with a $\chi 2$ test. A Student's t-test was used for comparisons between two groups. Differences in cell proliferation distributions were analyzed using a two-way analysis of variance (ANOVA) test. $p < 0.05$ was considered statistically significant.

3. Results

3.1 CIgG is frequently expressed in PCa and CIgG transcripts with unique patterns of VHDJH rearrangements are found in prostate cancer cells.

CIgG mRNA levels were significantly higher in PCa samples than in adjacent normal samples (Fig. 1A). We performed IHC to investigate CIgG protein expression in prostate tissues. IHC analysis indicated that CIgG staining in tumor tissues was mostly cytoplasmic in basal cells, Furthermore, we explored the staining profile of CIgG in normal prostate tissue. All 5 cases of benign prostate hyperplasia exhibited weak or negative CIgG staining when compared with that in the prostate cancer tissues (Fig. 1B), Moreover, among all the specimens, CIgG staining was stronger in specimens with either high Gleason score ($p = 0.044$) or advanced clinical stage($p = 0.027$) (Fig. 1C-F).

To determine whether IgG was produced by the cancer cells themselves or was obtained by extracellular uptake, we determined the transcription of IgG heavy chain in LNcap, PC3 and DU145 cells by RT-PCR using primers for both constant and variable regions. The results showed that the transcript of IgG heavy chain was significantly expressed in the three cancer cell lines (Fig. 1G, Figure S1, Table S4). Subsequently, the sequence features of these VHDJH rearrangements were analyzed via comparison with the best matching functional germline IgVH, IgDH and IgJH genes. The results clearly revealed that, like the B-Igs, all CIgG transcripts displayed classical and functional VHDJH rearrangement patterns. However, unlike B cell-derived IgVH, which has great diversity, several sets of VHDJH rearrangements were frequently present in the cell lines and even shared among different the cell lines, IGHV4-30/IGHD4-11/IGHJ4 were observed in 8/8 in PC3 cell samples; IGHV3-7/IGHD3-10/IGHJ5 were observed in 5/8 in DU145 samples; IGHV3-15/IGHD3-3/IGHJ4 were observed in 4/8 in LNcap samples. The prostate cancer-VHDJH rearrangements showed restricted VH, DH, and JH usage and unique VHDJH patterns, such as VH3 which was frequently present (16/24 VHDJH rearrangements analyzed in this study), especially VH3-7, which was expressed in DU145 (5/8), and LNcap (2/8) cells; moreover, among germline IGHJ1-6 genes, only IGHJ4 (16/24) and IGHJ5 (8/24) were frequently expressed, however, IgDH showed diversity in each cell line, DH4-11 rearrangement was observed in PC3 cells; DH3-10, DH2-15 and DH1-26 were observed in DU145 cells; and DH3-3, DH2-21 and DH5-12 were observed in LNcap cells. (Fig. 1G, Figure S1, Table S4). In addition, to enhancing IgG affinity, B cell-derived IgVH of IgG was usually hypermutated. Thus, we

analyzed the mutation pattern in prostate cancer-derived IgVH, and compared the sequence homology among VHDJH rearrangements from three cancer cell lines. We found that prostate cancer-derived IgVH only showed a low frequency of mutation (Fig. 1G, Figure S1, Table S4). Furthermore, the same mutated points were frequently shown among different VHDJH rearrangements, resulting in high homology between VHDJH rearrangements in IgVH (Fig. 1G, Figure S1, Table S4). The results suggested that the conserved domain of IgVH as well as that of IgHJ4 and IgHJ5 may support the common functions of different VHDJH rearrangements in prostate cancer cells, but IgDH determines the unique biological activity of each VHDJH rearrangement.

3.2 ClgG is essential for the anchorage of cancer cells to the extracellular matrixand and for cell-cell adhesion, and knockdown of IgG reduces the proliferation, migration and invasion of prostate cancer cells

To investigate the functional relevance of ClgG-mediated induction of the malignant phenotype in prostate cancer cell lines, we performed cell migration and invasion assays. We found that ClgG knockdown resulted in an obvious reduction in the migratory, invasive and proliferative ability of cells (Fig. 2A-D). Conversely, prostate cancer cells with ectopic ClgG expression had increased cell migration and invasion (Fig. 2E and 2F).

Next, we performed animal studies to investigate the influence of ClgG on tumor growth in vivo. The in vitro results were supported, BALB/c nude mice that were administered subcutaneous injections of PC3 and DU145 cells with ClgG knockdown had significantly reduced tumor volme and weights compared with those in mice injected with prostate cancer cells carrying the empty vector (Fig. 2G-J).

3.3. Cigg Cells Displayed More Csc-like Characteristics

To further analyze whether $ClgG^{high}$ cells have CSClike characteristics, we performed colony formation, sphere formation and drug-resistance assays to determine their proliferation, selfrenewal and drug-resistance abilities in vitro. PC3 cells with $ClgG^{high}$ expression displayed significantly higher colony forming and sphere forming efficiency and greater resistance to paclitaxel than $ClgG^{-/low}$ cells (Fig. 3A-C). To confirm that $ClgG^{high}$ cells have tumor initiating abilities, $ClgG^{high}$ and $ClgG^{-/low}$ cells purified from PC3 cells were used to perform tumorigenicity assays in NOD/SCID mice. As few as 500 purified $ClgG^{high}$ cells showed higher tumor formation ability than $ClgG^{-/low}$ cells (Fig. 3D). Tumors were observed in 50% (3/6) of the $ClgG^{-/low}$ mice compared to 83.3% (5/6) of the $ClgG^{high}$ mice. Moreover, tumor volume and weight in the $ClgG^{-/low}$ group were lower than those in the $ClgG^{high}$ group (Fig. 3D-E).

3.4. Cigg Is An Ar-repressed, Adt-inducible Gene

Interestingly, we analyzed another set of samples that consist of tissue specimens from 5 patients with prostate cancer before and after receiving ADT, collected from Peking University People`s Hospital (Beijing, China). CIgG was increased in prostate tumors from patients who had undergone ADT compared with the corresponding levels in the same patients before ADT treatment (Fig. 4A-B). Moreover, CIgG was significantly elevated in the prostate PDX model subjected to castration in the GEO prostate cancer datasets (Fig. 4C). We also found that cells treated with the AR ligand DHT had lower levels of CIgG, and this effect occurred in a dose-dependent manner (Fig. 4D).

Cytoplasmic CIgG was increased in prostate tumors from patients who had received ADT compared to those from patients before ADT treatment. In addition, we found that AR-negative PC3 and DU145 cells, which readily metastasize to bone[19, 20], had higher CIgG expression levels than cell lines that do not metastasize, such as AR-positive LNCaP, and C4-2 (Fig. 4E)

To assess whether the abundance of CIgG was mediated by ADT, we validated the expression of CIgG in AR-positive LNCaP and C4-2 cells relative to the AR signaling response. In AR^+ LNCaP and C4-2 cells, transient ablation of androgen led to increases in both mRNA and protein expression of CIgG (Fig. 4F-H); moreover, LNcap cells treated with the AR ligand DHT had lower levels of CIgG, and the downregulated expression could be rescued by the addition of the AR antagonist ARN509 (Fig. 4I); in addition, C4-2 cells treated with ARN509 showed upregulated CIgG expression (Fig. 4J). All these data indicate that AR itself is a repressor of CIgG expression.

To further confirm the biological function of AR on CIgG, we performed a luciferase reporter assay. The relative luciferase signals from the reporter plasmid into which the CIgG gene promoter had been inserted were significantly reduced by cotransfection with the AR plasmid (Fig. 4K).

3.5 CIgG associates with SOX2 expression and contributes to CRPC NE progression

It has been suggested that AR directly represses SOX2 in castration-resistant prostate cancer cell lines [21], The mean expression correction was validated in TCGA prostate cancer datasets, showing that SOX2 mRNA expression correlates inversely with AR (Fig. 5A-B). Our AR chromatin-IP first showed that AR binds the SOX2 promoter in castration-sensitive LNcap cell line (Fig. 5C). In addition, we found that AR knockdown was able to increase the expression of SOX2 (Fig. 5E). SOX2 is a critical TF that has been implicated in resistance to antiandrogen therapy [22, 23]. We hypothesized that CIgG stimulates malignant progression through the upregulation of SOX2 after ADT. CIgG expression was positively associated with SOX2 expression, as confirmed with TCGA prostate cancer datasets (Fig. 5D). We next examined whether CIgG abundance is upregulated by SOX2 in prostate cancer cell lines. Using SOX2-specific siRNA in C4-2 and DU145 cells, we observed a reduction in CIgG (Fig. 5F).

Taken together, the data demonstrate that CIgG can be induced by ADT though SOX2.

Here, we observed that knockdown of CIgG in C4-2, and DU145 cells consistently led to a decrease in the phosphorylation levels of MAPK/ERK and AKT (Fig. 5H). The data suggest that CIgG promotes MAPK/ERK and AKT activation. MEK/ERK and AKT signaling pathways play an important role in treatment resistance to facilitate PCa progression to CRPC[14, 24]. Moreover, MAPK/ERK and AKT are well-known drivers of CRPC[13, 15], and NSE, an NEPC (neuroendocrine prostate cancer) marker, levels decrease as well (Fig. 5H). These findings suggest CIgG-mediated MAPK/ERK and AKT activation as a mechanism of resistance to antiandrogen therapy.

Western blot analysis corroborated that the expression of E-cadherin (CDH1), a protein negative-related to tumor invasion, was clearly increased, and the expression of proteins positiverelated to tumor invasion, such as N-cadherin, vimentin and snail, was reduced (Fig. 5G) by CIgG knockdown.

We also examined the effect of RP215 on established xenograft models Following injection of RP215 at 5 mg/kg around the tumor, we observed significant inhibition of the growth of the treated tumors compared with that of control tumors treated with mIgG. At the termination of the experiment, the size and weight of tumors in the RP215 treated group were significantly lower than those in control group, and IHC analyses showed that RP215 inhibitor-treated tumors had reduced CIgG, pERK, pAKT and vimentin expression (Fig. 5I-L).

4. Discussion

In prostate cancer, resistance to hormone deprivation therapy is currently the major hurdle in treatment. Next-generation ARPIs (androgen receptor pathway inhibitors), such as ENZ and ABI have marginal efficacy[25], which is usually accompanied by reactivation of AR signaling or shifting of the phenotypes to anaplastic and NE carcinomas that are devoid of AR activity[26]. In efforts to develop more effective therapies, it is critical to improve the understanding of the molecular mechanisms underlying the development of CRPC.

SOX2 is a well-defined transcription factor that supports the proliferation and invasiveness of prostate cancer[27], A previous study suggested that AR directly represses SOX2 in an AR-positive castration-resistant prostate cancer cell line [21]; in addition, our data confirmed this finding in a castration-sensitive prostate cancer cell line (Fig. 5C); this indicates that, that genes elevated only in CRPC are mainly involved in the aggressive growth of CRPC, However, the expression of potential CRPC driver genes elevated not only sustains CRPC but also initiates CRPC, as known CRPC driver genes are typically: (1) be upregulated in CRPC, (2) show elevated expression prior to, and during, the progression from hormone-naive prostate cancer (HNPC) to CRPC; and (3) are functionally essential for CRPC development[16], We obtained evidence that SOX2-CIgG fulfills the criteria above for CRPC drivers.

Elevated SOX2 expression can be induced due to loss of AR-mediated repression during castration. Herein, SOX2 was shown to promote castration-resistance, lineage plasticity and NE differentiation in

prostate cancer[22, 28, 29]. We hypothesize that the ADT-induced SOX2-CIgG pathway is involved in the therapeutic resistance and progression of prostate cancer. These findings suggest that induction of CIgG is associated with increased malignancy in vitro and in vivo and neuroendocrine marker expression (NSE), suggesting that CIgG might act as a vital regulator in CRPC development. Data from human specimens highlighted the clinical relevance of CIgG in aggressive prostate cancer tumors(Fig. 1C-F), This result is consistent with previous findings that CIgG gene expression in prostate cancer is related to cell differentiation and clinical status[30]. We also found that CIgG activation drives malignant progression and lineage plasticity in prostate cancer by activating MAPK/ERK and AKT pathways, which have been reported to be critical for CRPC development and progression[13–16]. Thus, targeting CIgG, a potential upstream mediator of MAPK/ERK and AKT (Fig. 6), with its monoclonal antibody RP215 may improve the current treatment of CRPC.

Our results also confirm that CIgG could promote epithelial-mesenchymal transition (EMT) in prostate cancer cell lines, which is dependent on the activation of AKT, and MAPK/ERK. This result is consistent with previous findings.[31, 32]. In addition, SOX2 as a stem-like transcription factor could promote EMT[32, 33]. Therefore, our findings provide a molecular bridge by which SOX2 promotes the progression of prostate cancer, suggesting a critical role for CIgG in the development of CRPC (Fig. 6).

5. Conclusion

Our results show that a high level of CIgG is associated with ADT resistance and that RP215 can specifically block the pro-oncogenic properties of CIgG. Thus, our study highlights the potential for the development of a new therapy for CRPC patients by providing a rationale for the use of RP215, the monoclonal antibody of CIgG, to combat therapeutic resistance.

Declarations

6. Acknowledgements

Not applicable.

7. Authors` contributions

In this work, Caipeng Qin and Zhengzuo Sheng conceived and carried out experiments; Xinmei Huang, Jingshu Tang and Yang Liu conceived experiments and analyzed data; Tao Xu and Xiaoyan Qiu designed the protocol. All authors read, edited and approved the final manuscript

8. Funding

This study was supported by grants from the National Natural Science Foundation of China (31671469).

9.Availabilith of data and materials

All data presented or analyzed in this study are included either in this article or in the additional files.

10.Ethics approval and consent to participate

This study was approved by the Ethics Committee of Peking University People`s Hospital, Beijing, China.

11.Consent for publication

All authors have consented to publication of the results presented in this manuscript

12.Competing interests

The authors have no conflicts of interest to declare.

References

1. Scher HI, Fizazi K, Saad F, Taplin ME, Sternberg CN, Miller K, et al. Increased survival with enzalutamide in prostate cancer after chemotherapy. N Engl J Med. 2012;367(13):1187–97.
2. Ryan CJ, Smith MR, de Bono JS, Molina A, Logothetis CJ, de Souza P, et al. Abiraterone in metastatic prostate cancer without previous chemotherapy. N Engl J Med. 2013;368(2):138–48.
3. Qiu X, Zhu X, Zhang L, Mao Y, Zhang J, Hao P, et al. Human epithelial cancers secrete immunoglobulin g with unidentified specificity to promote growth and survival of tumor cells. Cancer Res. 2003;63(19):6488–95.
4. Chen Z, Gu J. Immunoglobulin G expression in carcinomas and cancer cell lines. Faseb j. 2007;21(11):2931–8.
5. Chen Z, Huang X, Ye J, Pan P, Cao Q, Yang B, et al. Immunoglobulin G is present in a wide variety of soft tissue tumors and correlates well with proliferation markers and tumor grades. Cancer. 2010;116(8):1953–63.
6. Liu Y, Liu D, Wang C, Liao Q, Huang J, Jiang D, et al. Binding of the monoclonal antibody RP215 to immunoglobulin G in metastatic lung adenocarcinomas is correlated with poor prognosis. Histopathology. 2015;67(5):645–53.
7. Babbage G, Ottensmeier CH, Blaydes J, Stevenson FK, Sahota SS. Immunoglobulin heavy chain locus events and expression of activation-induced cytidine deaminase in epithelial breast cancer cell lines. Cancer Res. 2006;66(8):3996–4000.
8. Zheng J, Huang J, Mao Y, Liu S, Sun X, Zhu X, et al. Immunoglobulin gene transcripts have distinct VHDJH recombination characteristics in human epithelial cancer cells. J Biol Chem.

2009;284(20):13610–9.

9. Hu D, Duan Z, Li M, Jiang Y, Liu H, Zheng H, et al. Heterogeneity of aberrant immunoglobulin expression in cancer cells. Cell Mol Immunol. 2011;8(6):479–85.
10. Lee G. Cancer cell-expressed immunoglobulins: CA215 as a pan cancer marker and its diagnostic applications. Cancer Biomark. 2009;5(3):137–42.
11. Tang J, Zhang J, Liu Y, Liao Q, Huang J, Geng Z, et al. Lung squamous cell carcinoma cells express non-canonically glycosylated IgG that activates integrin-FAK signaling. Cancer Lett. 2018;430:148–59.
12. Liao Q, Liu W, Liu Y, Wang F, Wang C, Zhang J, et al. Aberrant high expression of immunoglobulin G in epithelial stem/progenitor-like cells contributes to tumor initiation and metastasis. Oncotarget. 2015;6(37):40081–94.
13. Bitting RL, Armstrong AJ. Targeting the PI3K/Akt/mTOR pathway in castration-resistant prostate cancer. Endocr Relat Cancer. 2013;20(3):R83–99.
14. Kinkade CW, Castillo-Martin M, Puzio-Kuter A, Yan J, Foster TH, Gao H, et al. Targeting AKT/mTOR and ERK MAPK signaling inhibits hormone-refractory prostate cancer in a preclinical mouse model. J Clin Invest. 2008;118(9):3051–64.
15. Li S, Fong KW, Gritsina G, Zhang A, Zhao JC, Kim J, et al. Activation of MAPK Signaling by CXCR7 Leads to Enzalutamide Resistance in Prostate Cancer. Cancer Res. 2019;79(10):2580–92.
16. Hao J, Ci X, Xue H, Wu R, Dong X, Choi SYC, et al. Patient-derived Hormone-naive Prostate Cancer Xenograft Models Reveal Growth Factor Receptor Bound Protein 10 as an Androgen Receptor-repressed Gene Driving the Development of Castration-resistant Prostate Cancer. Eur Urol. 2018;73(6):949–60.
17. Sheng Z, Liu Y, Qin C, Liu Z, Yuan Y, Hu F, et al. IgG is involved in the migration and invasion of clear cell renal cell carcinoma. J Clin Pathol. 2016;69(6):497–504.
18. Sheng Z, Liu Y, Qin C, Liu Z, Yuan Y, Yin H, et al. Involvement of cancer-derived IgG in the proliferation, migration and invasion of bladder cancer cells. Oncol Lett. 2016;12(6):5113–21.
19. Chen WY, Tsai YC, Yeh HL, Suau F, Jiang KC, Shao AN, et al. Loss of SPDEF and gain of TGFBI activity after androgen deprivation therapy promote EMT and bone metastasis of prostate cancer. Sci Signal. 2017;10(492).
20. Chang YS, Chen WY, Yin JJ, Sheppard-Tillman H, Huang J, Liu YN. EGF Receptor Promotes Prostate Cancer Bone Metastasis by Downregulating miR-1 and Activating TWIST1. Cancer Res. 2015;75(15):3077–86.
21. Kregel S, Kiriluk KJ, Rosen AM, Cai Y, Reyes EE, Otto KB, et al. Sox2 is an androgen receptor-repressed gene that promotes castration-resistant prostate cancer. PLoS One. 2013;8(1):e53701.
22. Mu P, Zhang Z, Benelli M, Karthaus WR, Hoover E, Chen CC, et al. SOX2 promotes lineage plasticity and antiandrogen resistance in TP53- and RB1-deficient prostate cancer. Science. 2017;355(6320):84–8.

23. Yu X, Cates JM, Morrissey C, You C, Grabowska MM, Zhang J, et al. SOX2 expression in the developing, adult, as well as, diseased prostate. Prostate Cancer Prostatic Dis. 2014;17(4):301–9.
24. Sarker D, Reid AH, Yap TA, de Bono JS. Targeting the PI3K/AKT pathway for the treatment of prostate cancer. Clin Cancer Res. 2009;15(15):4799–805.
25. Yuan X, Cai C, Chen S, Chen S, Yu Z, Balk SP. Androgen receptor functions in castration-resistant prostate cancer and mechanisms of resistance to new agents targeting the androgen axis. Oncogene. 2014;33(22):2815–25.
26. Bluemn EG, Coleman IM, Lucas JM, Coleman RT, Hernandez-Lopez S, Tharakan R, et al. Androgen Receptor Pathway-Independent Prostate Cancer Is Sustained through FGF Signaling. Cancer Cell. 2017;32(4):474 – 89.e6.
27. Bae KM, Su Z, Frye C, McClellan S, Allan RW, Andrejewski JT, et al. Expression of pluripotent stem cell reprogramming factors by prostate tumor initiating cells. J Urol. 2010;183(5):2045–53.
28. Labrecque MP, Coleman IM, Brown LG, True LD, Kollath L, Lakely B, et al. Molecular profiling stratifies diverse phenotypes of treatment-refractory metastatic castration-resistant prostate cancer. J Clin Invest. 2019;130:4492–505.
29. Bishop JL, Thaper D, Vahid S, Davies A, Ketola K, Kuruma H, et al. The Master Neural Transcription Factor BRN2 Is an Androgen Receptor-Suppressed Driver of Neuroendocrine Differentiation in Prostate Cancer. Cancer Discov. 2017;7(1):54–71.
30. Liu Y, Chen Z, Niu N, Chang Q, Deng R, Korteweg C, et al. IgG gene expression and its possible significance in prostate cancers. Prostate. 2012;72(6):690–701.
31. Chen X, Xiong X, Cui D, Yang F, Wei D, Li H, et al. DEPTOR is an in vivo tumor suppressor that inhibits prostate tumorigenesis via the inactivation of mTORC1/2 signals. Oncogene. 2020;39(7):1557–71.
32. Wang K, Ji W, Yu Y, Li Z, Niu X, Xia W, et al. FGFR1-ERK1/2-SOX2 axis promotes cell proliferation, epithelial-mesenchymal transition, and metastasis in FGFR1-amplified lung cancer. Oncogene. 2018;37(39):5340–54.
33. Laughney AM, Hu J, Campbell NR, Bakhoum SF, Setty M, Lavallee VP, et al. Regenerative lineages and immune-mediated pruning in lung cancer metastasis. Nat Med. 2020;26(2):259–69.

Figures

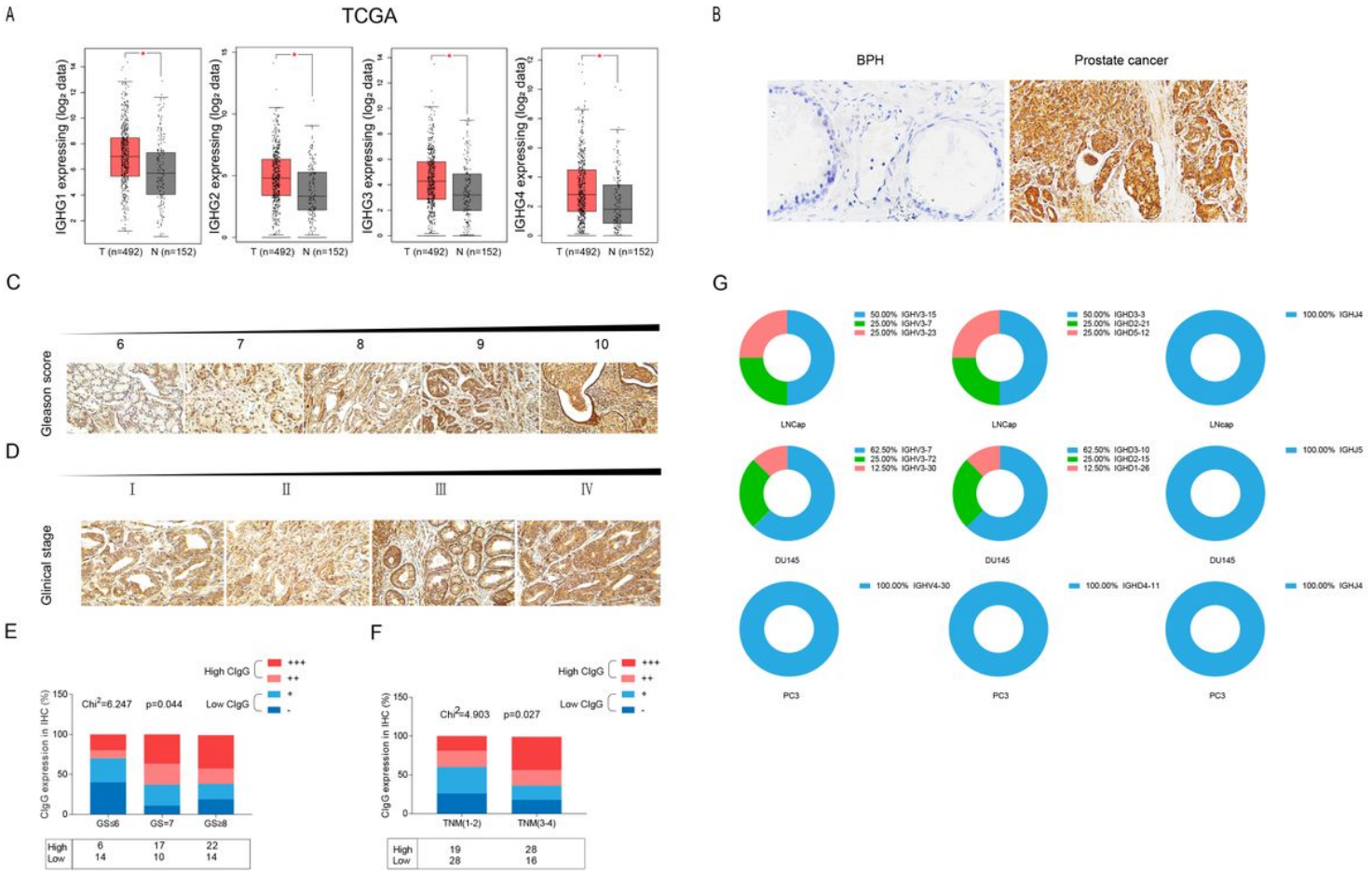

Figure 1

CIgG expression in prostate cancers. (A)IGHG1-4 (immunoglobulin heavy constant gamma 1-4) mRNA expression in of prostate cancer tissue, and paired normal tissues was derived from TCGA data set ((*: p < 0.05). (B-D) IHC analysis of CIgG expression in BPH and prostate cancer tissue samples. The correlation between CIgG expression and Gleason score and TNM stages was analyzed using a chi-squared test(E-F). (G)The prostate cancer cell lines sequences carrying these VHDJH rearrangements were analyzed by comparison with the best matching functional germline IgVH, IgDH and IgJH genes, VHDJH usage is summarized.

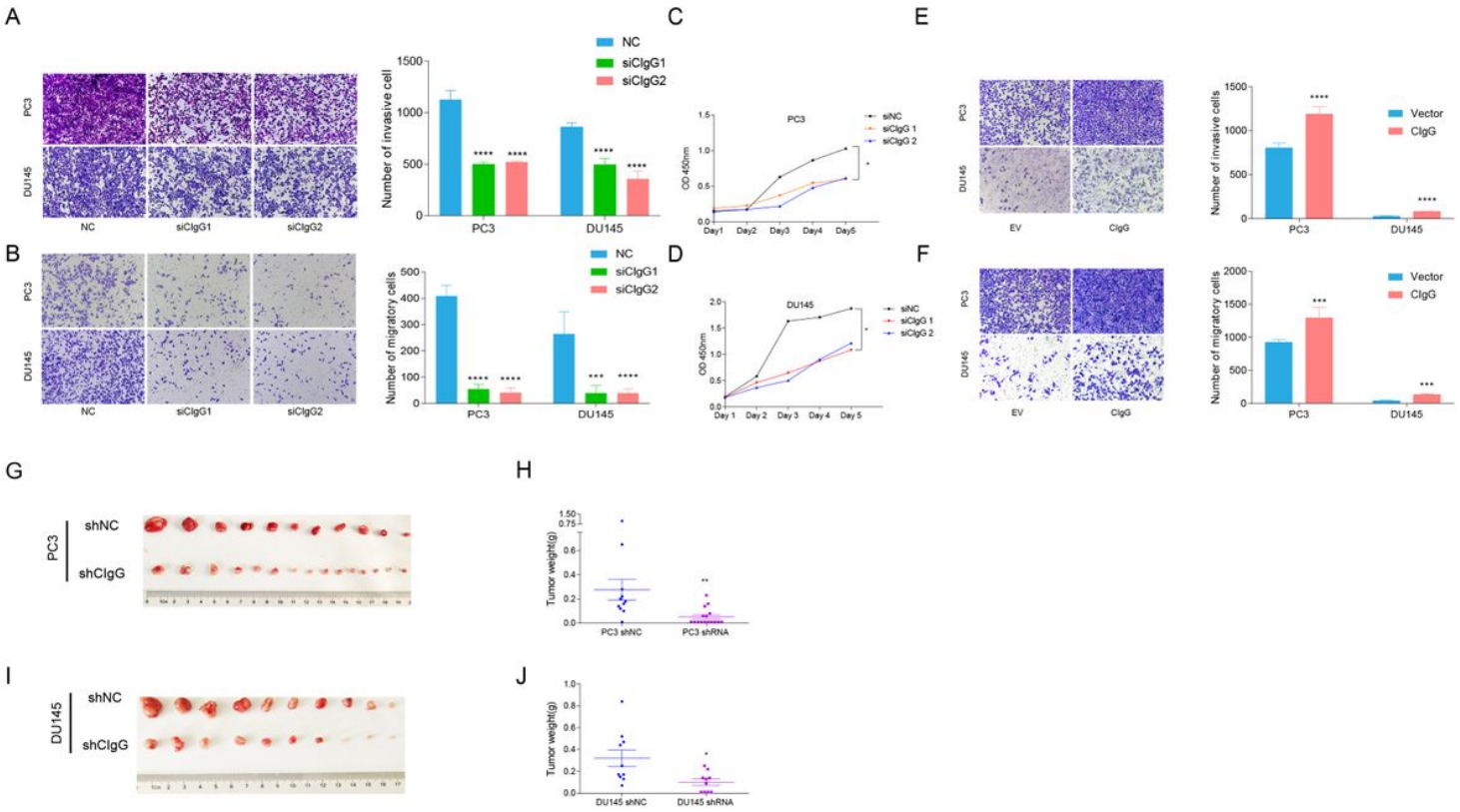

Figure 2

ClgG induces malignant progression of prostate cancer cells. Transwell invasion assays treated with (A) or without (B) Matrigel showed that ClgG deletion suppressed migration and invasion in PC3 and DU145 cells. Cell proliferation was measured using CCK-8 (C-D), Transwell invasion of PC3 and DU145 cells transfected with the EV or ClgG-expressing vector(E-F). The volume and weight of PC3 and DU145-derived xenografts in the ClgG-silenced (shClgG) and control (shNC) groups(G-J). Data from the migration, invasion, and proliferation assays are presented as the mean±SEM from three independent experiments, (* $p < 0.05$; ** $p < 0.01$; *** $p < 0.001$; **** $p < 0.0001$).

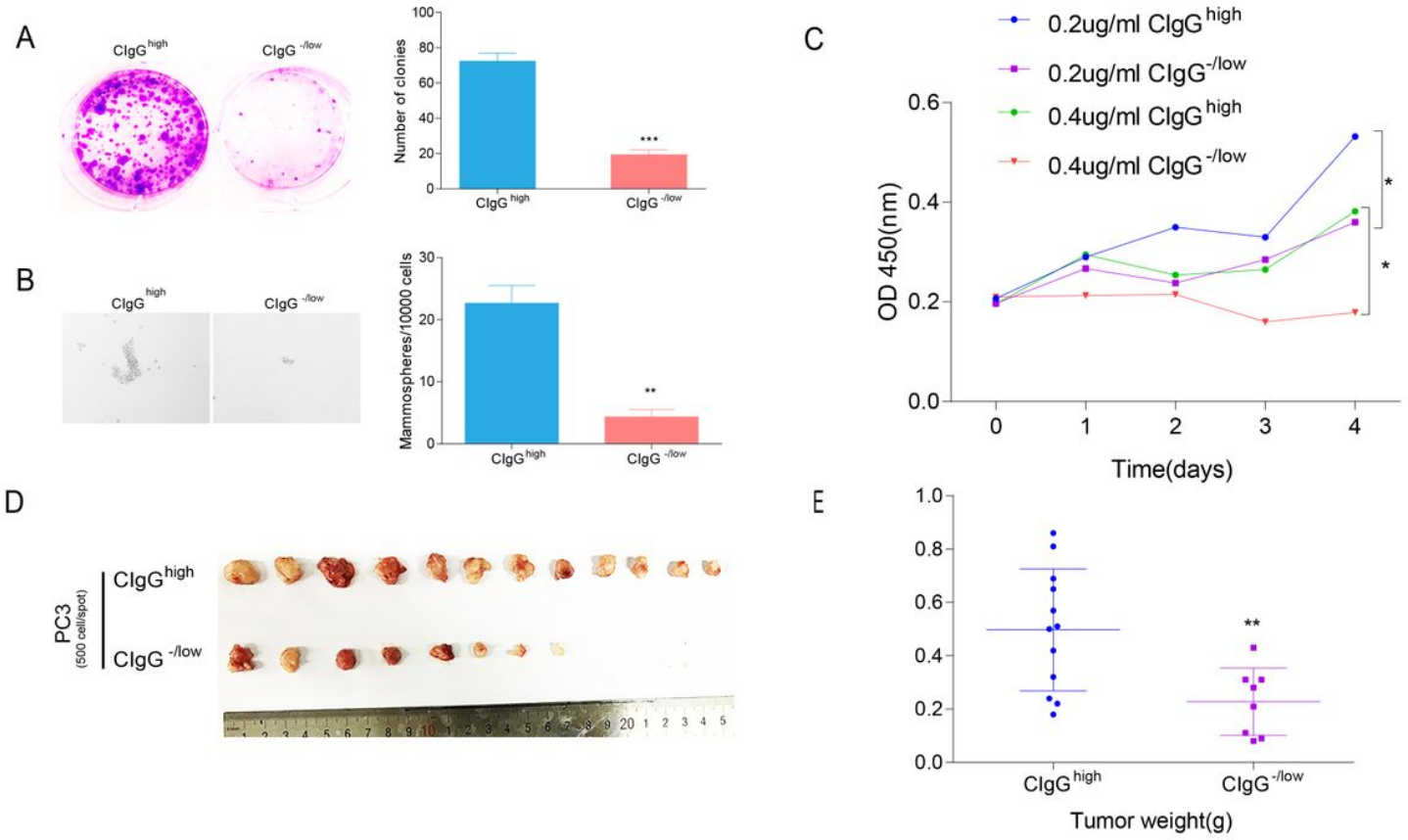

Figure 3

CIgGhigh prostate cancer cells displayed high CSC-like characteristics. Proliferation of CIgG high PC3 cells sorted by FACS was detected by clone formation assay(A). Mammospheres were generated from 10,000 CIgG high PC3 cells in suspension culture, and then counted(B). The drug resistance capacity of CIgG−/low and CIgG high PC3 cells to paclitaxel was analyzed by CCK8 assay(C). Images (D), and weights (E) of tumor xenografts in NOD/SCID mice 5 weeks after subcutaneous inoculation with CIgG−/low and CIgG high PC3 cells with 500 cells/spot. Data from the colony formation and mammosphere assays are presented as the mean±SEM from three independent experiments, (* $p < 0.05$; ** $p < 0.01$; *** $p < 0.001$).

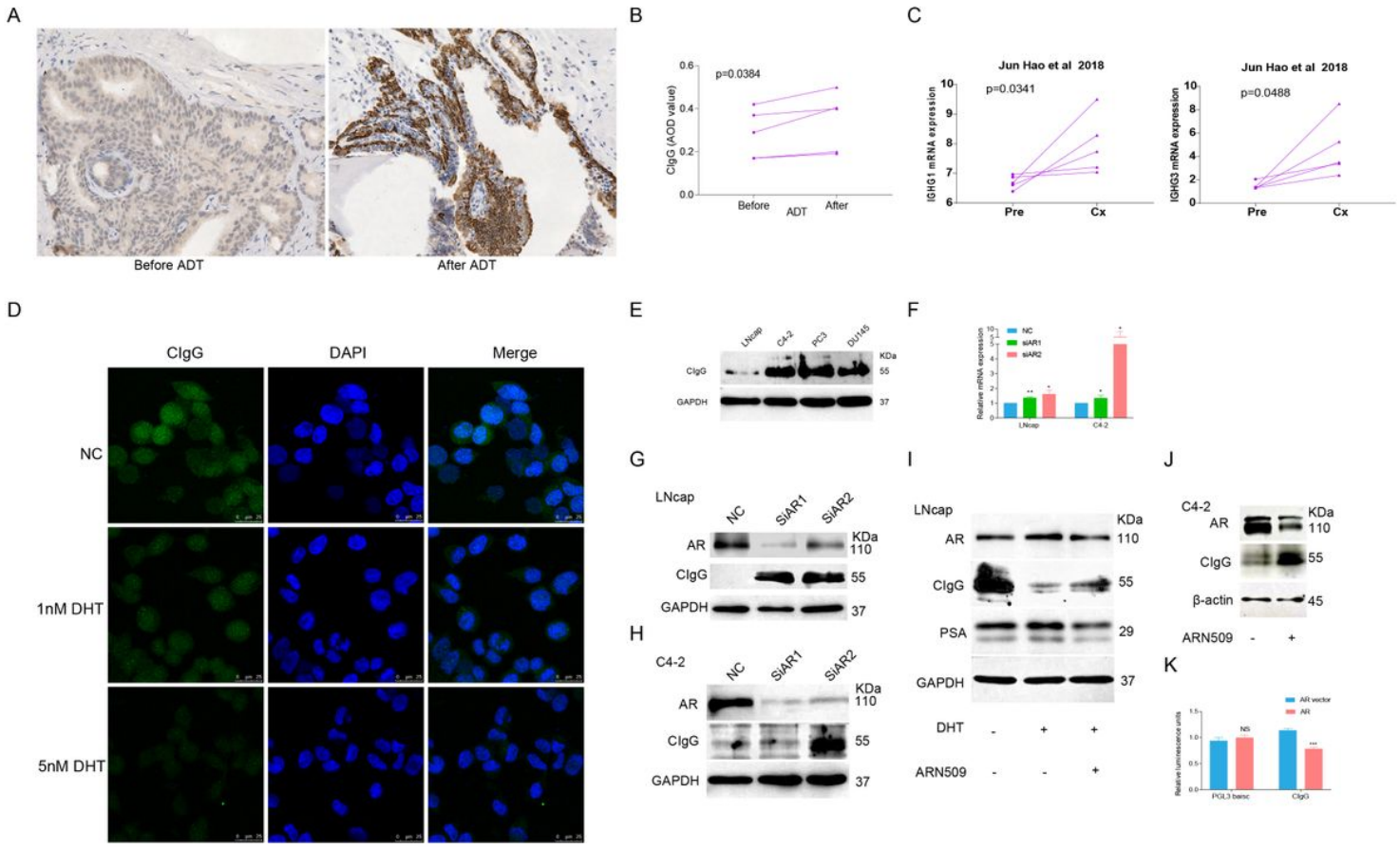

Figure 4

ADT induces ClgG expression Another 5 patient-matched Pre-ADT biopsies and 5 post-ADT prostatectomy specimens were detected by immunohistochemistry(A-B). ClgG mRNA expression in intact and castrated prostate PDX models constructed by Jun Hao al [16](C). The effects of DHT on the expression of ClgG(D). Western blotting of ClgG from a panel of prostate cancer cells(E). Effects of androgen signal inhibition on ClgG expression in LNCaP and C4-2 cells were determined by qRT-PCR and Western blotting(F-H). For some cultures, 10 nM AR ligand DHT with or without 5 μM ARN509, an AR inhibitor, was added for 24 h (I-J). Transcriptional inhibitory functions of AR as indicated by reduced luciferase reporter activity. Luminescence units were normalized using Renilla luciferase signal(K). Data from the qPCR, and luciferase assays are presented as the mean±SEM from three independent experiments, (* $p < 0.05$; ** $p < 0.01$; *** $p < 0.001$).

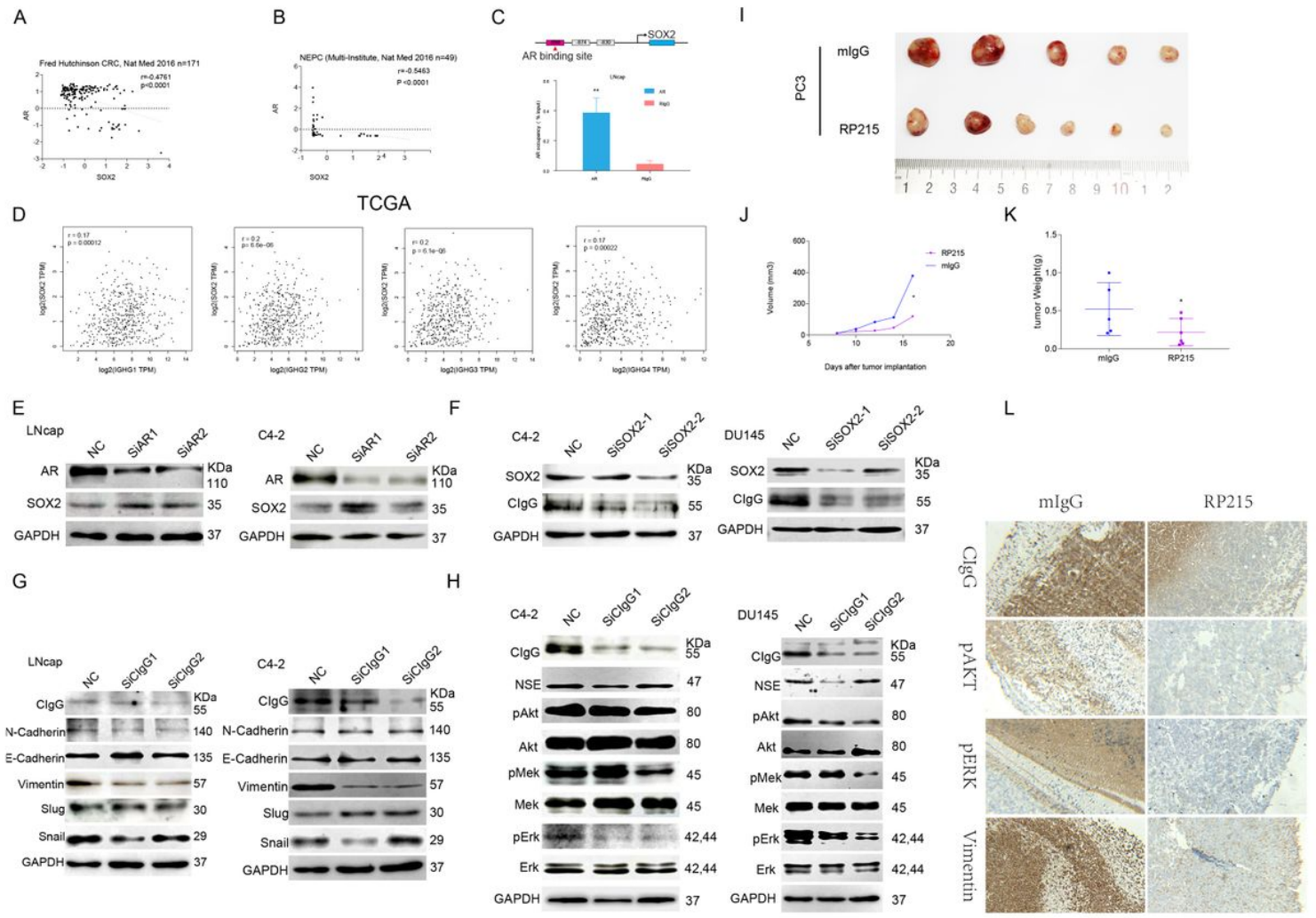

Figure 5

SOX2 is positively associated with the induction of ClgG, and ClgG knockdown reduces MAPK/ERK and AKT activity in PCa cells and inhibits EMT. Spearman correlation analysis of SOX2 with AR in clinical tissue samples from TCGA prostate cancer datasets(A-B). Significance was determined using a two-tailed test. AR chromatin immunoprecipitation (ChIP) documents direct binding of AR to the SOX2 enhancer region and enrichment of the SOX2 promoter after AR ChIP was normalized as a percentage of total chromatin input. IgG served as a negative control. When compared to total input, AR significantly enriched for the SOX2 enhancer ($p<0.05$); Data represent three independent experiments(C). Spearman correlation analysis of ClgG with SOX2(D). Western blot analysis of relationship of AR, SOX2 and ClgG(E-F). the effects of ClgG knockdown on phosphorylated AKT, MEK and ERK levels and EMT were determined using ClgG knockdown (SiClgG1 and SiClgG2) and control (NC) cell lines(G-H). Babl/c nude mice bearing PC3 tumors were injected with 5 mg/kg of RP215 or mIgG every other day around the tumor. Growth curves (J) images (I) and weight plots (K) of harvested tumors at the end of the assay. IHC staining of subcutaneous tumors with antibodies specific for ClgG, pAKT, pERK, and vimentin in tumor-bearing mice from L. Data from ChIP assays are presented as the mean±SEM from three independent experiments, (* $p < 0.05$; ** $p < 0.01$; *** $p < 0.001$).

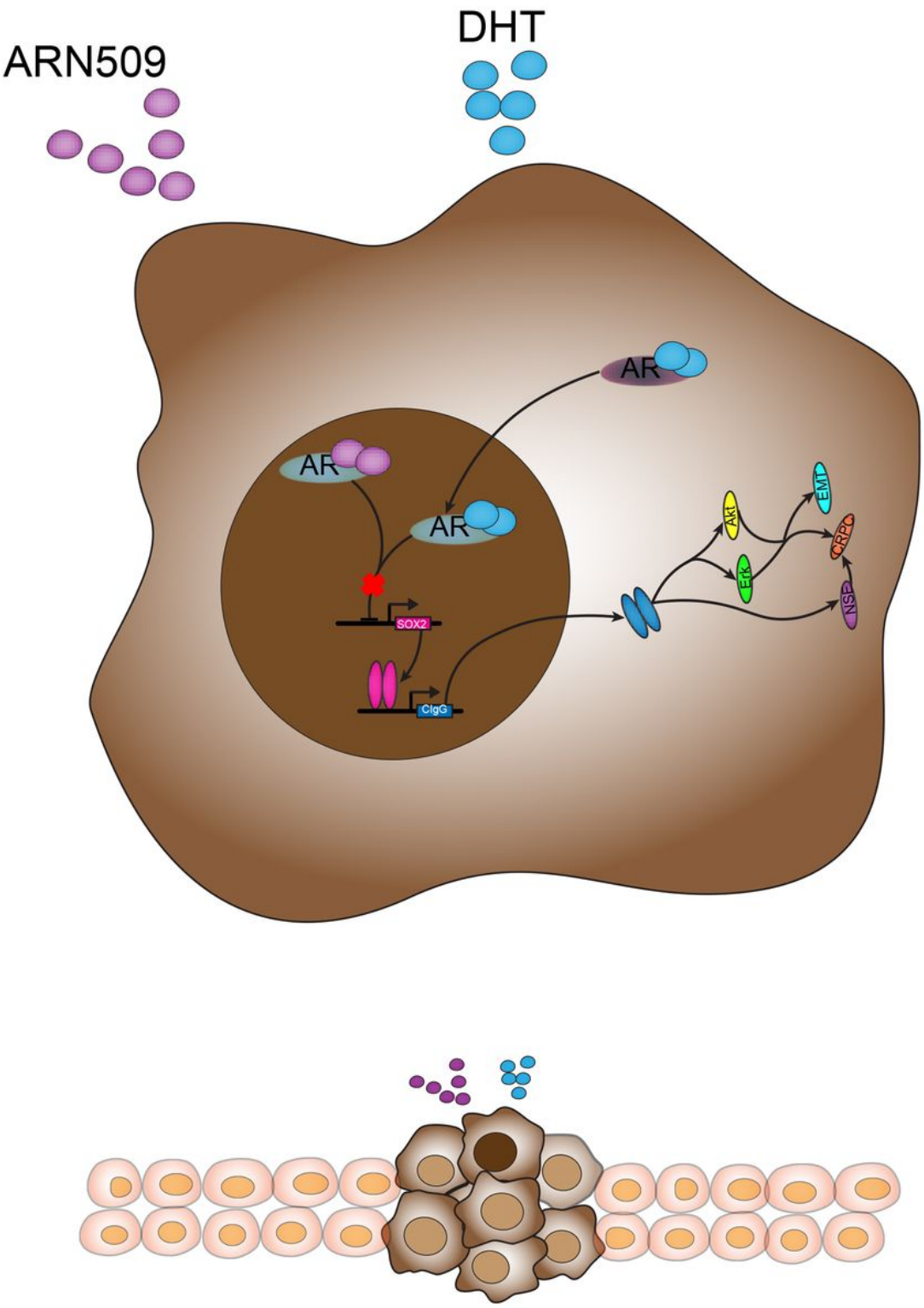

Figure 6

Proposed model of ClgG-mediated malignant phenotype of prostate cancer. An anti-androgen or AR antagonist inactivates AR signaling and induces ClgG expression. ClgG upregulation enhances malignant progression and is involved in the development of CRPC via the activated of AKT and the MARK/ERK pathway.

Supplementary Files

This is a list of supplementary files associated with this preprint. Click to download.

- Supplementary.docx